JOURNAL OF JICIVILTECH
INNOVATIONS IN CIVIL ENGINNERING AND TECHNOLOGY

e-ISSN 2687-2129
jiciviltech, ***2022***, *4(2), 61-75*

Araştırma Makalesi / Research Article

Buckling of Square and Circular Perforated Square Plates under Uniaxial Loading

*[1]Fethullah USLU, [2]Mustafa Halûk SARAÇOĞLU, [3]Uğur ALBAYRAK

[1]Kütahya Dumlupınar University, Faculty of Engineering, Department of Civil Engineering, Kütahya, Türkiye, fethullah.uslu@dpu.edu.tr, ORCID ID: http://orcid.org/0000-0001-8057-5119
[2]Kütahya Dumlupınar University, Faculty of Engineering, Department of Civil Engineering, Kütahya, Türkiye, mhaluk.saracoglu@dpu.edu.tr, ORCID ID: http://orcid.org/0000-0003-3842-5699
[3]Eskişehir Osmangazi University, Faculty of Engineering and Architecture, Department of Civil Engineering, Eskişehir, Türkiye, albayrak@ogu.edu.tr, ORCID ID: http://orcid.org/0000-0001-7326-3213

Geliş / Recieved: 18.10.2022; Kabul / Accepted: 10.11.2022

Abstract

This paper aims to investigate the critical buckling loads of uniaxially loaded simply supported square thin plates with central circular and square holes in terms of some parameters like hole shapes, slenderness ratios and total hole areas. In this study, buckling analyses of perforated plates with different hole shapes of perforation and slenderness ratios were carried out. For this purpose, plate models with seven different total hole areas were examined together with the non-perforated plate. The total hole area ratios in the models are 0.79%, 3.14%, 7.07%, 12.57%, 19.63%, 28.27% and 38.48%, respectively. The total hole areas of the models with square holes are arranged to be the same as the models with circular holes to compare the results among circular and square perforated plates properly. The models were established by using the finite-element (FE) software ANSYS using Shell-181 elements which are 4-node structural shell elements. The comparisons on critical buckling loads between square and circular perforated results show that the buckling load for the plates with square holes is higher than for the plates with circular holes.

Keywords: *Buckling, Perforated plates, Finite element, Square perforated, Circular perforated*

*[1]Sorumlu yazar / Corresponding author

Bu makaleye atıf yapmak için
Uslu, F, Saraçoğlu, M. H. & Albayrak, U. (2022). Buckling of Square and Circular Perforated Square Plates under Uniaxial Loading. *Journal of Innovations in Civil Engineering and Technology (JICIVILTECH), 4(2),* 61-75.

Tek Eksenli Yükleme Altındaki Kare ve Dairesel Delikli Kare Plakların Burkulması

Öz

Bu makale, merkezi dairesel ve kare deliklere sahip tek eksenli yüklü basit mesnetli kare ince plakların kritik burkulma yüklerini delik şekilleri, narinlik oranları ve toplam delik alanları gibi bazı parametreler açısından incelemeyi amaçlamaktadır. Bu çalışmada, farklı delik şekillerine ve narinlik oranlarına sahip delikli plakların burkulma analizleri yapılmıştır. Bu amaçla boşluksuz plak ile beraber yedi farklı boşluk oranına sahip plak modelleri incelenmiştir. Modellerdeki boşluk oranları sırasıyla %0.79, %3.14, %7.07, %12.57, %19.63, %28.27 ve %38.48 şeklindedir. Dairesel ve kare delikli plaklar arasındaki sonuçları doğru bir şekilde karşılaştırabilmek için kare delikli modellerin toplam delik alanları, dairesel delikli modellerle aynı olacak şekilde düzenlenmiştir. Modeller, kütüphanesinde bulunan 4 düğüm noktalı yapısal kabuk elemanı olan Shell-181 elemanları kullanılarak sonlu elemanlar yazılımı ANSYS ile analiz edilmiştir. Elde edilen sonuçlar, aynı boşluk alanına sahip kare delikli plakaların burkulma yüklerinin dairesel delikli plakalara göre daha yüksek olduğunu göstermiştir.

Anahtar kelimeler: *Burkulma, Delikli plaklar, Sonlu eleman, Kare delik, Dairesel delik.*

1.Introduction

Perforated plates are used in many engineering areas as a structural member and are subjected to a wide variety of loads. One of these loads is the buckling load which was acting in-plane uniaxial compressive to these members. Buckling behavior is often encountered in such structures and commonly generates large deformations. Therefore, buckling design for perforated plates used as the main structural member is gaining considerable importance in the structural designs.

In this sense, although there are studies on perforated plates, there has not been much research on buckling and there are few studies on this subject in the literature. There were also studies about perforated rectangular and square plates subjected to various loads as lateral bending and inplane tension loads with different boundary conditions (Albayrak & Saraçoğlu, 2016; Saraçoğlu & Albayrak, 2018; Saraçoğlu et al., 2020; Saraçoğlu et al., 2021, Karakaya, 2022).

Narayanan and Avanessian (1984), investigated stability of plates with cut-outs plates under shear by using finite element method. They computed buckling coefficient for simply and fixed supported plates containing various shaped cut-outs. After the calculations they suggested a formula for the use of practical engineers. Brown, presented elastic stability analyses of perforated plates with different aspect ratios for concentrated loading. He emphasizes in his study that some simple modifications to the boundary conditions and geometry of the plate affect the critical load of the plate majorly (Brown, 1990). Shakerley and Brown (1996), studied buckling of square eccentrically positioned perforated plates with fully fixed and simply supported boundaries. They explained the effect of longitudinal or lateral slots and the location of perforations to the critical buckling load in their study. Shanmugam et al. (1999) have proposed critical loads for the design of perforated plates with different boundary conditions and different shapes of openings which are subject to uni-axial and bi-axial in-plane compressive loadings for design in their study. El-Sawy et al. (2004) have investigated the buckling stress of circular perforated rectangular and square plates subjected to uniaxial loadings. By using the finite element method effects of various parameters have been determined in their study. Maiorana et al. (2008) have investigated the stability of perforated plates with rectangular and circular holes under localized symmetric loads. Kömür and Sönmez (2008), were studied the stability of rectangular plates with different perforations and loading cases, different normalized hole sizes, and aspect ratios by using finite element software program ANSYS. Rezaeepazhand and Sabori (2008), were studied the damaged metallic perforated square plates and they conducted finite element codes for numerical studies. Maiorana et al. (2009) were were developed some numerical non-linear analyses for perforated plates with eccentric holes in their parametric study. In perforated plates, Komur (2011) selected elliptical holes as a different geometrical shape and he

investigates the effect of some parameters on buckling behavior. Seifi et al. (2017) were studied the global buckling behavior of reinforced perforated plates experimentally and numerically. Al-Amar and Al-Araji (2017) were investigated the buckling of perforated and unperforated stiffened plates under uniaxial compressive load. Yanli et al. (2019) investigated the buckling behavior of perforated plates under bending by using finite element software and a practical formula was proposed for the coefficient of buckling. Soares et al., (2019) studied about the buckling of perforated thin and thick plates. Investigated plates were considered with the simply supported boundary condition and loaded with uni axial in-plane loads. And also they compare the results with the literature. Soleimanian et al. (2020) studied the buckling and vibration of perforated plates made with composite materials under thermal loads and they suggested a model for analyses. Guo and Yao (2021) presented an extensive parametric study about the buckling behavior of perforated plates with rectangular and circular hole shapes. Evaluated plates have been considered as simply supported and investigated with different parameters in their study. Kim et al. (2021) were investigated the perforated plates subjected to uni axial compression loadings by using the commercial finite element analysis program and experimentally. They were considered thickness, aspect ratio and opening size as variables in their study. Silveira et al. (2021) were studied about perforated plate buckling which has elliptical-shaped holes. They numerically simulated the models with software using the Finite Element Method and square steel perforated plates have a symmetric geometry. Plates were simply supported in its four edges and submitted to a biaxial compressive load and has a centered elliptical cutout. They apply the constructal design method for numerical analysis of the perforated plates. Fu and Wang (2022) were investigated the buckling of perforated plates and for this purpose, they developed a new semi-analytical model by using the Timoshenko shear beam theory in their study and they compare the results with finite element method solutions.

The main objective of this study is to investigate the critical buckling loads of simply supported perforated plates with different perforations and different slenderness ratios under in-plane uniaxial compressive loads numerically. Investigated plates have the same opening sizes with different hole shapes; circular, and square shaped.

2.Material and Methods

Plates can be unstable because of the critical in-plane forces acting on the plates and these forces have effects also on flexural behavior. And also, these plates acting with these forces may undergo buckling by becoming unstable. In engineering practice design for stability is critical. If the in-plane load acting on the square plate is below the critical value and too small to cause buckling, the state of equilibrium is stable. But if the in-plane load is greater than the critical value, the state of

equilibrium is unstable, and this leads to larger deflections.

The general deflection expression which satisfies the boundary conditions of a simply supported rectangular plate can be expressed as an infinite series of as follows:

$$w = \sum_{m=1,2,\cdots}^{\infty} \sum_{n=1,2,\cdots}^{\infty} a_{mn} \sin\frac{m\pi x}{a} \sin\frac{n\pi y}{b} \quad (1)$$

In equation (1) w defines the deflection value. This general expression can be customized for a simply supported rectangular plate uniformly lateral loaded in the x direction and carrying a concentrated load P at a point with coordinates ζ and η is as follows.

$$w = \frac{4P}{ab\pi^4 D} \sum_{m=1,2,3,\cdots}^{\infty} \sum_{n=1,2,3,\cdots}^{\infty} \frac{sin\frac{m\pi\zeta}{a} sin\frac{n\pi\eta}{b}}{\left(\frac{m^2}{a^2}+\frac{n^2}{b^2}\right)-\frac{m^2\sigma_{cr}h}{\pi^2 a^2 D}} sin\frac{m\pi x}{a} sin\frac{n\pi y}{b} \quad (2)$$

In equation (2) D is the plate flexural rigidity, a is the length of the plate in x axis, b is the length of the plate in y axis, and σ_{cr} is the critical stress value.

When the denominator of one of the terms in equation (2) becomes equal to zero the critical stress value σ_{cr} occurs. This critical value will occur when n=1 in equation (2). Equation (3) and Equation (4) give these critical stress values.

$$\sigma_{cr} = \frac{\pi^2 a^2 D}{hm^2}\left(\frac{m^2}{a^2}+\frac{1}{b^2}\right)^2 \quad (3)$$

$$\sigma_{cr} = \frac{\pi^2 D}{hb^2}\left(\frac{mb}{a}+\frac{a}{mb}\right)^2 \quad (4)$$

Geometry of a plate model subjected to uniaxial compressive forces is shown in Figure 1.

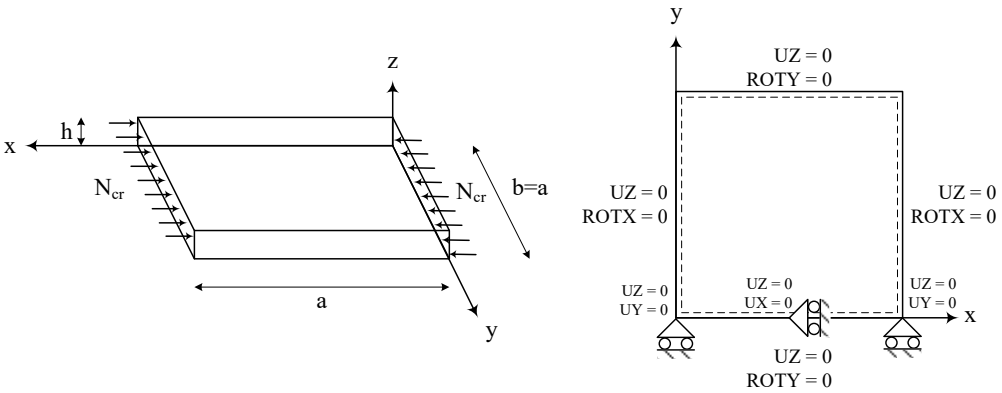

Figure 1. Non-perforated plate model and boundary conditions under uniaxial compressive forces

The elastic critical stress of a square plates subjected to uniform axial compressive stress which are simply supported along all edges is as follows (Bryan, 1891; Guo & Yao, 2021):

$$\sigma_{cr} = k\frac{\pi^2 E}{12(1-\nu^2)(a/h)^2} \quad (5)$$

In equation (5) E is the elastic modulus, ν is the Poisson's ratio, a is the plate width and h is the plate thickness. Plate buckling coefficient is expressed in equation (5) as k. If D is the plate flexural rigidity (Timoshenko & Woinowsky-Krieger, 1959), plate buckling coefficient is explained in equation (6) and equation (7).

$$k = \sigma_{cr}\frac{ha^2}{D\pi^2} \quad (6)$$

$$D = \frac{Eh^3}{12(1-\nu^2)} \quad (7)$$

The calculation results of the examples discussed in this study were obtained using the ANSYS finite element package program. The 4-node structural shell element SHELL 181 from the ANSYS element library, shown in Figure 2, is used as the finite element. The SHELL 181 element is 4-node structural shell element with different options such as triangular option, membrane option or layered option. Each of the 4 nodes of this element has six degrees of freedom: translations in the x, y, and z directions and rotations in the x, y, and z axes.

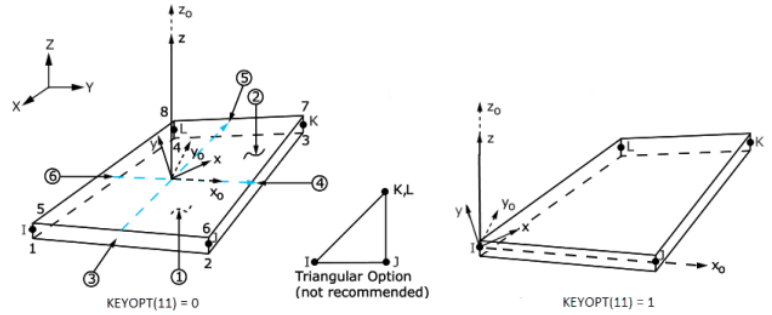

Figure 2. Geometry of SHELL181 finite element in ANSYS (Swanson Analysis System Inc., 2005)

It supports properties such as linear, large rotation, and large strain nonlinear applications (Swanson Analysis System Inc., 2005).

3.Examples

In order to investigate the hole shape effect on buckling of uniaxially loaded square plates, one dimension of the plate is taken as 300 mm, and analyses were performed for non-perforated, square perforated, and circle perforated square plates. Investigated two plates have different hole shapes with the same opening sizes. Holes on the plates are circular, and square shaped.

Geometry and boundary conditions of the plate model with a circular hole is shown in Figure 3. In the present study, plates are considered to be simply supported on all edges. Freedom of the translational displacement in the plane of the plate and condition of nonoccurrence of rigid body movement should be applied to the models. For this purpose, two joints at the bottom corners were fixed in the y direction and middle joint at the bottom edge was fixed in the x direction.

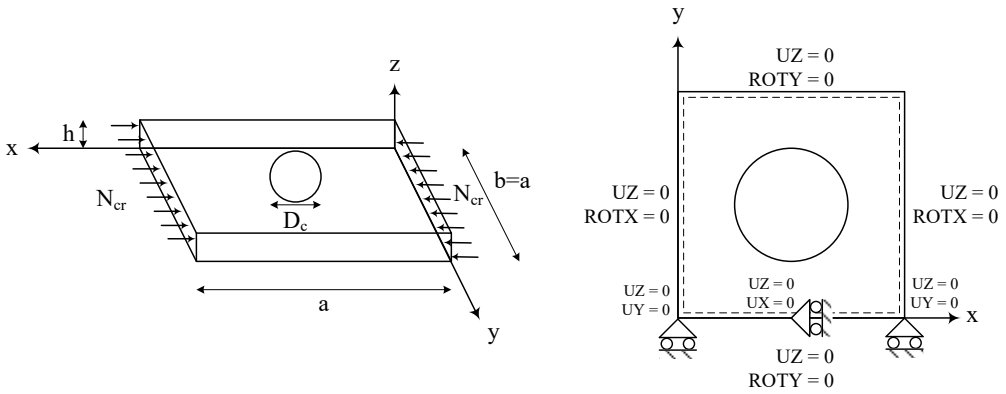

Figure 3. Plate model with a circular hole and boundary conditions.

Dimensions and the loading of the plate is shown in Figure 1 and Figure 3 Material properties of the example plates were modulus of elasticity (E) and Poisson's ratio (ν) are 200000 MPa, and 0.3, respectively.

3.1 Verification of Mesh Quality

The results obtained in numerical simulations performed by the finite element method are dependent on the mesh quality. Results obtained with a poor mesh structure will also give poor or inaccurate results. Therefore, it is necessary to make sure that the mesh is good enough to obtain reliable results. In general, the finer mesh means the more accurately results. But in this case, there are more data points, and the number of nodes and unknowns will increase. To determine the dependence of the results on the mesh quality a mesh independence study is performed.

In this mesh quality study, buckling analyses were performed on a simply supported square steel plate with the dimension 300 mm x 300 mm and a thickness of 2 mm. A series of models were generated for this sample plate by meshing with finite elements whose size was varying from 50 mm (coarsest mesh) to 2 mm (finest mesh) divisions for mesh quality verification. Critical buckling load yielded from each model were calculated and compared to study the influence of mesh quality on the buckling analysis results. This series of buckling analysis results, comparisons and percentage approximate errors were calculated by comparing other results to the exact results (Timoshenko & Woinowsky-Krieger, 1959) and shown in Figure 4. It can be observed from Figure 4 that when the number of mesh elements along plate length is higher than 60, the increase of mesh density does not significantly improve the accuracy of critical buckling load anymore.

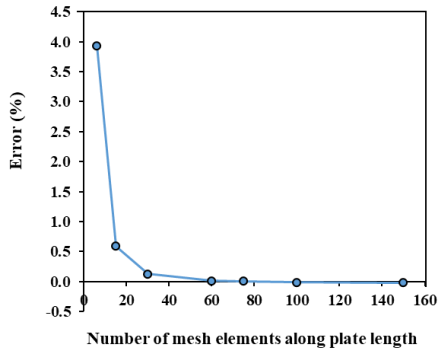

Figure 4. Number of mesh elements vs accuracy for critical buckling load

Different results are obtained with different finite element frequencies created for the analyzed plate models. Because the mesh created for the problems in the finite element method directly affects the results. As the number of elements increases, more accurate results are approached. The frequency of elements more than necessary will cause different numerical errors. In order to determine the correct finite element mesh density, the relationship between element size and critical buckling load is examined by increasing the number of finite elements, and the element size with the same amount of critical buckling load can be determined. As a result of such convergence processes, the finite element size is taken as 5 mm in the problems solved in this study.

3.2 Verification of Finite Element Analysis Models

The correct calculation of the analysis results is directly dependent on the selected element type as well as the finite element mesh density. To evaluate the accuracy of finite element solutions, the obtained results should be compared with experimental results or theoretical values. In this study, in order to verify the finite element solutions, the problems taken from the reference samples were also solved and the convergence of the obtained values was checked.

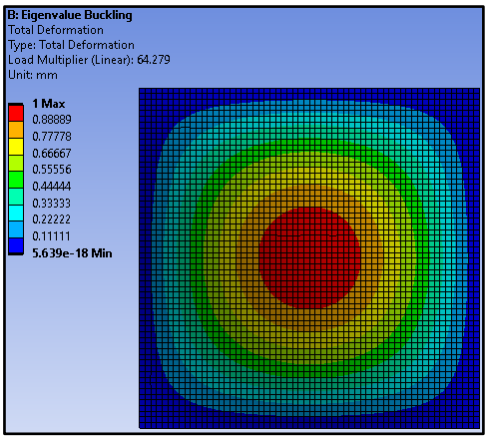

Figure 5. Contour plot of total deformations for a non-perforated plate.

Before investigating the buckling behavior of the perforated plates by using finite element software buckling analyses of the non-perforated plates taken from the literature were performed by using the program to verify the accuracy. For this purpose, the results obtained by finite element method are compared to those results obtained by using an exact solution procedure based on the infinite power series (Timoshenko & Woinowsky-Krieger, 1959). As an example, buckling

analysis was performed for non-perforated square plate by taking the finite element size as 5mm and the contour plot of total deformations of the plate is shown in Figure 5.

Buckling analyses of the other example problems also performed by using the finite-element software and critical buckling loads were obtained.

The buckling coefficient is calculated as in Equation (8).

$$N_{cr} = k\frac{D\pi^2}{b^2} \quad (8)$$

In equation (8) N_{cr} is the critical buckling load. The buckling coefficients obtained by the finite element for the simply supported square plates without holes with different thickness and the corresponding values obtained from Timoshenko and Woinowsky-Krieger (Timoshenko & Woinowsky-Krieger, 1959) are listed in Table 1. Length of square steel plate is taken as 300 mm.

Table 1. Comparison of critical buckling load and buckling coefficients of non-perforated plate

a/h	N_{cr}^{FE} (N/mm)	k^{FE}	$N_{cr}^{(Tim.\&Woi.)}$ (N/mm)	$k^{(Tim.\&Woi.)}$	$k^{Difference\%}$	$N_{cr}^{Difference\%}$
150	64.2790	4.0005	64.2709	4.0000	0.013	0.013
100	216.8800	3.9994	216.9144	4.0000	-0.016	-0.016
50	1732.1000	3.9926	1735.3151	4.0000	-0.185	-0.185

Difference% values are calculated by the formula in equation (9):

$$\text{Difference\%} = \frac{\text{FE}-\text{Reference}}{\text{Reference}} \times 100 \quad (9)$$

It can be seen from the Table1 that there is a good consistency of the buckling coefficients and loads obtained from finite element method and numerical results from literature. These results indicate that the finite element method models presented in this paper is reliable and accurate. And also, critical buckling load for simply supported square plate with a circular hole is verified from El-Sawy and Nazmy (El-Sawy & Nazmy, 2001) and shown in Table 2. In the middle of the square plate, a circular hole is perforated, and the diameter was taken as 150mm which is half of the square plate length.

Table 2. Comparison of critical buckling load and buckling coefficients of a square plate with a circular hole

a/h	N_{cr}^{FE} (N/mm)	k^{FE}	$N_{cr}^{(El.\&Naz.)}$ (N/mm)	$k^{(El.\&Naz.)}$	$k^{Difference\%}$	$N_{cr}^{Difference\%}$
150	46.6390	2.9026	46.5964	2.9000	0.091	0.091
100	157.2800	2.9003	157.2629	2.9000	0.011	0.011
50	1253.9000	2.8903	1258.1034	2.9000	-0.334	-0.334

3.3 Finite Element Analysis Models

Analyzes were performed for square plates with a square, and circular hole of different open area ratios and different slenderness ratios (a/h = 50, 100, and 150). Plate surface areas are constant as 300 mm x 300 mm. Square plates with circular holes were taken as reference and the open area in each problem was modeled equally so that the sample problems could be compared with each other.

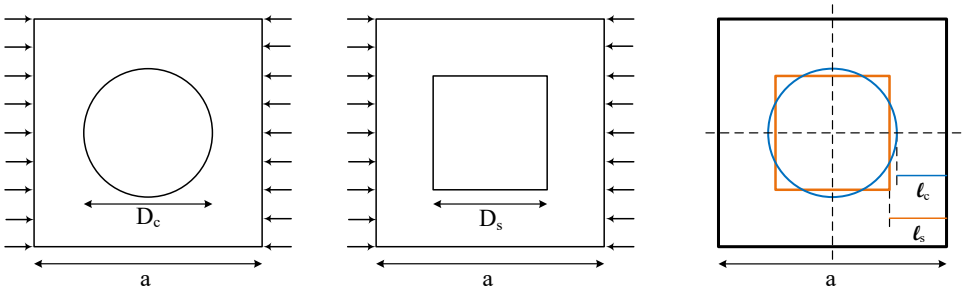

Figure 6. Plane view of square plate models with circle and square hole shapes.

A schematic plan view for one of the example problems which has the same open area is shown in Figure 6. The notation ℓ_s is the length between the line of action of the load and the square hole edge in the middle of the plate and the notation ℓ_c is the similar length for the circle hole.

Boundary conditions are simply supported in four edges as shown in Figure 1. A uniform unit load is applied to the edges of x=0 and x=a=300mm and performed the eigenvalue analysis by using the finite element software program. After obtaining the lowest eigenvalue, the critical buckling load N_{cr} was calculated. The effect of slenderness ratio, open area ratio, and hole shape on the critical buckling load of perforated square plates loaded with uniaxial compression are presented in Table 3. In the analyses, both cases of rectangular and circular holes in the middle of the plates are considered.

The variation of the length ℓ_s is for square perforated plate and the length lc for circle perforated plate versus the hole area is shown in Figure 7.

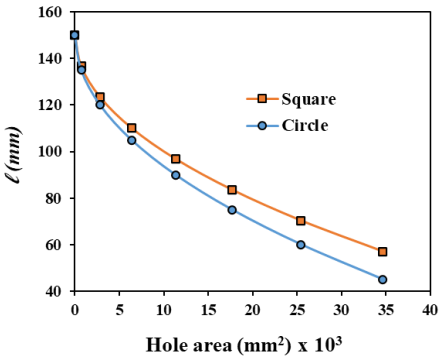

Figure 7. Variation of the location of the edge lines of the circular and square holes.

Figure 8 compares the critical buckling loads for simply supported square plates with square and circular holes. In this figure slenderness ratios of the plates are 150 so that 300 x 300 dimensioned plate thickness is 2 mm.

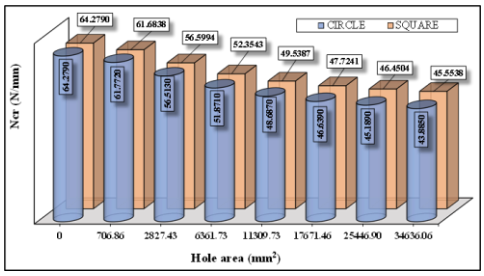

Figure 8. Critical buckling loads for perforated square plates (a/h=150).

In Figure 9 and Figure 10, the buckled shapes of the example plates are shown, indicating the formation of only one half-wave for all hole diameters used. In these seven example problems, the hole areas of the square holes are the same as the circle holes.

Table 3 Comparison of critical buckling loads with different parameters

Model no	h (mm)	Hole area (mm^2)	Open area ratio (%)	D_c (mm)	ℓ_c (mm)	N_{crc} (N/mm)	D_s (mm)	ℓ_s (mm)	N_{crs} (N/mm)
1	2	0.00	0.00	0	150	64.279	0.000	150.000	64.279
2	2	706.86	0.79	30	135	61.772	26.587	136.707	61.684
3	2	2827.43	3.14	60	120	56.513	53.174	123.413	56.599
4	2	6361.73	7.07	90	105	51.871	79.760	110.120	52.354
5	2	11309.73	12.57	120	90	48.687	106.347	96.826	49.539
6	2	17671.46	19.63	150	75	46.639	132.934	83.533	47.724
7	2	25446.90	28.27	180	60	45.189	159.521	70.240	46.450
8	2	34636.06	38.48	210	45	43.885	186.108	56.946	45.554
9	3	0.00	0.00	0	150	216.880	0.000	150.000	216.880
10	3	706.86	0.79	30	135	208.420	26.587	136.707	208.076
11	3	2827.43	3.14	60	120	190.680	53.174	123.413	190.882
12	3	6361.73	7.07	90	105	175.010	79.760	110.120	176.523
13	3	11309.73	12.57	120	90	164.240	106.347	96.826	166.967
14	3	17671.46	19.63	150	75	157.280	132.934	83.533	160.754
15	3	25446.90	28.27	180	60	152.300	159.521	70.240	156.329
16	3	34636.06	38.48	210	45	147.730	186.108	56.946	153.138
17	6	0.00	0.00	0	150	1732.100	0.000	150.000	1732.100
18	6	706.86	0.79	30	135	1664.600	26.587	136.707	1660.760
19	6	2827.43	3.14	60	120	1523.100	53.174	123.413	1522.322
20	6	6361.73	7.07	90	105	1397.900	79.760	110.120	1406.602
21	6	11309.73	12.57	120	90	1311.100	106.347	96.826	1328.598
22	6	17671.46	19.63	150	75	1253.900	132.934	83.533	1276.296
23	6	25446.90	28.27	180	60	1211.300	159.521	70.240	1237.184
24	6	34636.06	38.48	210	45	1169.600	186.108	56.946	1206.876

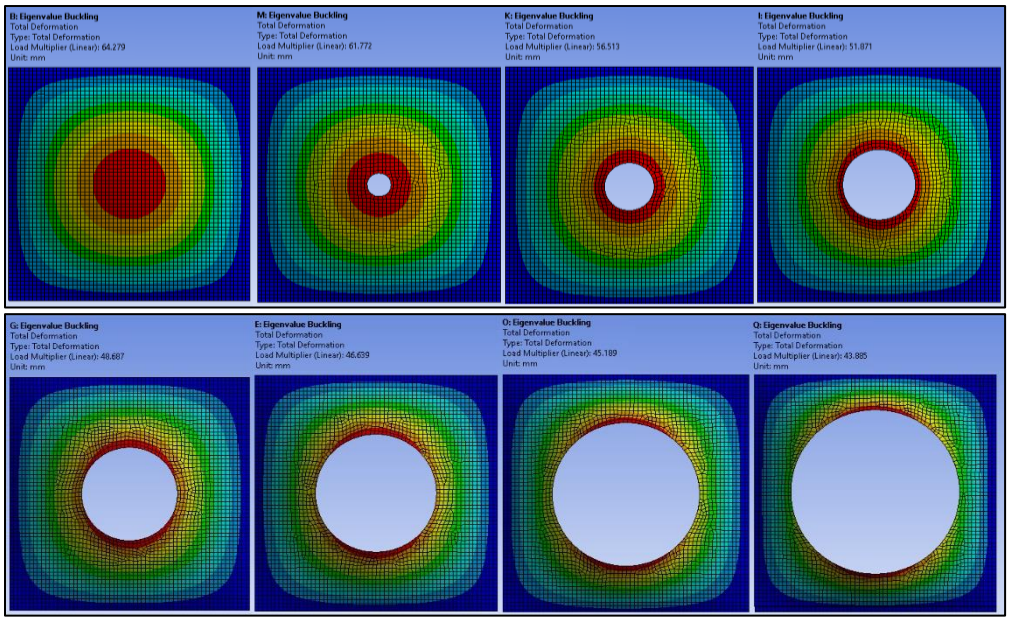

Figure 9. Buckling mode shapes for circle plate models with different hole areas.

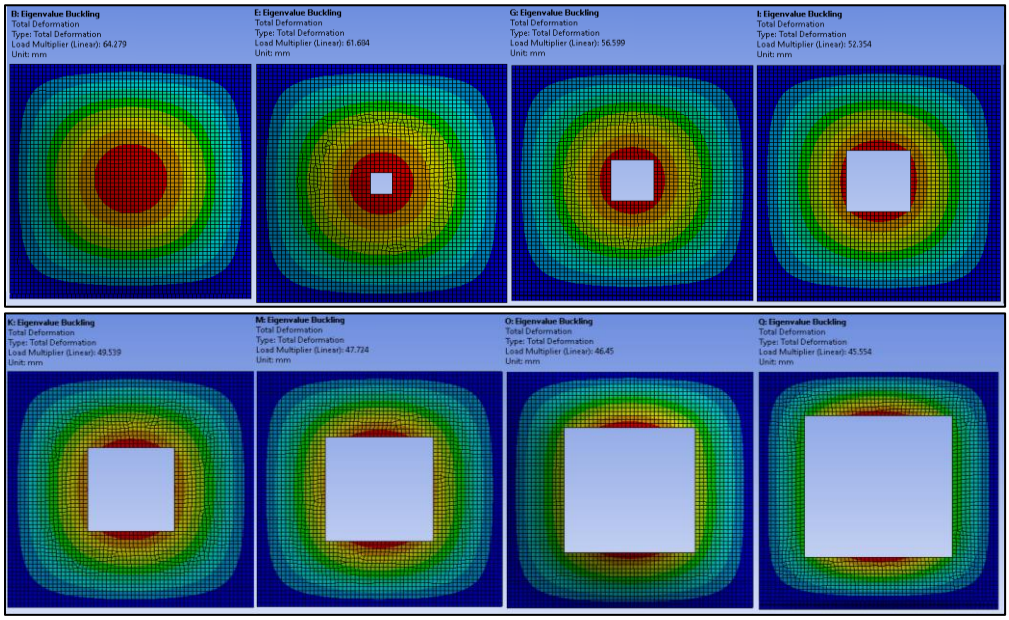

Figure 10. Buckling mode shapes for square plate models with different hole areas.

4.Results and Discussion

The critical buckling loads of simply supported different hole shaped perforated plates subjected to in-plane uniaxial compressive loads have been investigated numerically. Analyses were performed by using commercial finite element software package ANSYS. As a result of these simulations, it is observed

that when the hole area increases the critical buckling loads also decrease as expected. Because the plate rigidity was also decreased by the perforation.

In order to compare the results more accurately, the hole areas of the square-hole plates and the circular-hole plates were taken as the same. It is interesting that critical buckling loads of circular perforated plates are lower than the square perforated plates with the same hole area. Similar to what Brown et al. mentioned in their study (Brown et al., 1987), if the length between the line of action of the load and the hole edge in the middle of the plate is longer, this eventually increases the critical buckling load with the increased area between the edge of the square plate and the hole. Thus, the critical buckling load of a square hole plate is greater than for a circle hole plate which has the same boundary conditions and loadings.

As shown in Figure 7, the length ℓ_s is greater than the length lc for all considered example problems. As the hole area increases, the difference between the defined lengths increases, and accordingly the critical buckling loads for plates with square holes also increase. This result could be seen in detail in Figure 8 for the a/h ratio of 150. The graphs of critical buckling loads versus open hole areas for thicker plates with slenderness ratios of 100 and 50 are similar to this graph, but only the values of the loads change.

Analyses results of critical buckling loads for simply supported square plates with square and circle holes with the same hole ratio are shown in Figure 9 and Figure 10. It can be seen from the figures that when the hole area decreases total deformation of the plate increases especially at the edges of the holes. In the last two models whose hole area is larger, this value is more dominant at the edge of the hole perpendicular to the lines where uniaxial buckling loads are applied.

5.Conclusion

The critical buckling loads prediction of staggered arranged perforated plates with holes of different geometries stainless steel plates under compressive loading was investigated by finite element analysis software. For this purpose, buckling analyses of perforated plates with different hole shapes of perforation and slenderness ratios were carried out. Centrally located circular and square holes in square plates subjected to uniaxial buckling load have been considered and analyzed for simply supported boundary conditions.

The following are some conclusions that can be drawn based on the numerical outcomes of the problems:

- Increasing the size of the hole area will reduce the critical buckling load of simply supported perforated rectangular plates aforementioned in this study.
- As the hole area increases, the length between the action line of the uniaxial load and the circle hole edge in the middle of the plate decreases more than the length between the square hole edge.
- The critical buckling load of square and circular hole simply supported square plates with the same

hole area loaded with uniaxial buckling load is higher for plates with square holes than for plates with circular holes.

6.References

Albayrak, U., & Saraçoğlu, M. H. (2018). Analysis of Regular Perforated Metal Ceiling Tiles. International Journal of Engineering and Technology, 10(6), 440–446. doi: 10.7763/ijet.2018.v10.1099

Bader Al-Amar Mohammed S Hassan AL-Araji, Q. H. (2017). Buckling of Perforated and Unperforated Stiffened Plate. In Journal of Babylon University/Engineering Sciences.

Brown, C J. (1990). Elastic buckling of perforated plates subjected to concentrated loads. Computers and Structures, 36(6), 1103–1109.

Brown, Christopher J, Yettram, A. L., & Burnett, M. (1987). Stability of Plates with Rectangular Holes. Journal of Structural Engineering, 113(5), 1111–1116. doi: 10.1061/(ASCE)0733-9445(1987)113:5(1111)

Bryan, G. H. (1891). On the stability of a plane plate under thrusts in its own plane with applications to the buckling of the sides of a ship. Proceedings of London Mathematics Society, 54–67.

da Silveira, Thiago, Torres Pinto, V., Pedro Sarasol Neufeld, J., Pavlovic, A., Alberto Oliveira Rocha, L., Domingues dos Santos, E., & André Isoldi, L. (2021). Applicability evidence of constructal design in structural engineering: case study of biaxial elasto-plastic buckling of square steel plates with elliptical cutout. J. Appl. Comput. Mech, 7(2), 922–934. doi: 10.22055/JACM.2021.35385.2647

El-Sawy, K. M., & Nazmy, A. S. (2001). Effect of aspect ratio on the elastic buckling of uniaxially loaded plates with eccentric holes. Thin-Walled Structures, 39, 983–998. Retrieved from www.elsevier.com/locate/tws

El-Sawy, K. M., Nazmy, A. S., & Martini, M. I. (2004). Elasto-plastic buckling of perforated plates under uniaxial compression. Thin-Walled Structures, 42(8), 1083–1101. doi: 10.1016/J.TWS.2004.03.002

Fu, W., & Wang, B. (2022). A semi-analytical model on the critical buckling load of perforated plates with opposite free edges. Original Research Article Proc IMechE Part C: J Mechanical Engineering Science, 236(9), 4885–4894. doi: 10.1177/09544062211056890

Guo, Y., & Yao, X. (2021). Buckling Behavior and Effective Width Design Method for Thin Plates with Holes under Stress Gradient. doi: 10.1155/2021/5550749

Karakaya, C. (2022). Numerical investigation on perforated sheet metals under tension loading. Open Chemistry, 20(1), 244–253. doi: 10.1515/chem-2022-0142

Kim, J. H., Park, D. H., Kim, S. K., Kim, J. D., & Lee, J. M. (2021). Lateral deflection behavior of perforated steel plates: Experimental and numerical approaches. Journal of Marine Science and Engineering, 9(5). doi: 10.3390/jmse9050498

Komur, M. A. (2011). Elasto-plastic buckling analysis for perforated steel plates subject to uniform compression. Mechanics Research Communications, 38(2), 117–122. doi: 10.1016/J.MECHRESCOM.2011.01.001

Komur, M. A., & Sonmez, M. (2008). Elastic buckling of perforated plates subjected to linearly varying in-plane loading. Structural Engineering and Mechanics, 28(3), 353–356. doi: 10.12989/SEM.2008.28.3.353

Maiorana, E., Pellegrino, C., & Modena, C. (2008). Linear buckling analysis of perforated plates subjected to localised symmetrical load. Engineering Structures, 30(11), 3151–3158. doi: 10.1016/J.ENGSTRUCT.2008.04.024

Maiorana, E., Pellegrino, C., & Modena, C. (2009). Non-linear analysis of perforated

steel plates subjected to localised symmetrical load. Journal of Constructional Steel Research, 65(4), 959–964. doi: 10.1016/J.JCSR.2008.03.018

Narayanan, R., & der Avanessian, N. G. V. (1984). Elastic buckling of perforated plates under shear. Thin-Walled Structures, 2(1), 51–73. doi: 10.1016/0263-8231(84)90015-6

Rezaeepazhand, J., & Sabori, H. (2008). Buckling of perforated plates repaired with composite patches. Key Engineering Materials, 385–387, 377–380. Trans Tech Publications Ltd. doi: 10.4028/www.scientific.net/kem.385-387.377

Saraçoğlu, M. H., & Albayrak, U. (2016). Linear static analysis of perforated plates with round and staggered holes under their self-weights. Research on Engineering Structures & Materials, 2(1), 39–47. doi: 10.17515/resm2015.25me0910

Saraçoğlu, M. H., Uslu, F., & Albayrak, U. (2020). Stress and displacement analysis of perforated circular plates. Challenge Journal of Structural Mechanics, 6(3), 150. doi: 10.20528/cjsmec.2020.03.006

Saraçoğlu, M., Uslu, H., & Albayrak, F. (2021). Investigation of Hole Shape Effect on Static Analysis of Perforated Plates with Staggered Holes. International Journal of Engineering and Innovative Research, 3(2), 133–144. doi: 10.47933/ijeir.883510

Seifi, R., Chahardoli, S., & Akhavan Attar, A. (2017). Axial buckling of perforated plates reinforced with strips and middle tubes. Mechanics Research Communications, 85, 21–32. doi: 10.1016/J.MECHRESCOM.2017.07.015

Shakerley, T. M., & Brown, C. J. (1996). Elastic buckling of plates with eccentrically positioned rectangular perforations. International Journal of Mechanical Sciences, 38(8–9), 825–838. doi: 10.1016/0020-7403(95)00107-7

Shanmugam, N. E., Thevendran, V., & Tan, Y. H. (1999). Design formula for axially compressed perforated plates. Thin-Walled Structures, 34(1), 1–20. doi: 10.1016/S0263-8231(98)00052-4

Silveira, T., Neufeld, J. P. S., Rocha, L. A. O., Santos, E. D., & Isoldi, L. A. (2021). Numerical analysis of biaxial elasto-plastic buckling of perforated rectangular steel plates applying the Constructal Design method. IOP Conf. Ser.: Mater. Sci. Eng. doi: 10.1088/1757-899X/1048/1/012017

Soares Junior, R.A., Palermo Junior, L., & Wrobel, L.C. (2019). Buckling of perforated plates using the dual reciprocity boundary element method. In Boundary Elements and other Mesh Reduction Methods XLII (Vol. 126, pp. 89–100). WIT Press. doi: doi:10.2495/BE420081

Soleimanian, S., Davar, A., Jam, J. E., Zamani, M. R., & Beni, M. H. (2020). Thermal buckling and thermal induced free vibration analysis of perforated composite plates: a mathematical model. Mechanics of Advanced Composite Structures, 7, 15–23. doi: 10.22075/macs.2019.16556.1181

Swanson Analysis System Inc., A. (2005). ANSYS User's manual.

Timoshenko, S. , Woinowsky-Krieger, S. (1959). Theory of Plates and Shells. In McGraw-Hill, Inc. McGraw-Hill, Inc.

Yanli, G., Xiaoqing, S., Xiao, L., Xingyou, Y., Zhifan, X., Bin, X., Jianyi, S. (2019). Elastic buckling of thin plate with circular holes in bending. E3S Web of Conferences, 136, 3–8. doi: 10.1051/e3sconf/201913604043